A case study: Thermophysics characterization of tropical soils extracted in the horizons HA and HB

A. M. Picolloto[1], D. Kuritza[1], V.S. Zanuto[1], E. Cezar[2], M. R. Nanni[2], M. L. Baesso[1], A. C. Bento[1, *]

[1] Laboratório de Espectroscopia Fotoacústica e Fototérmica, Departamento de Física, universidade Estadual de Maringá, Maringá, Parana-Brasil.
[2] Laboratório de Solos e Nutrição de Plantas, Departamento de Agronomia, Universidade Estadual de Maringá, Maringá, Parana-Brazil.
*Corresponding authors: acbento@uem.br; angela.picolloto@gmail.com.

Received: 8 November, 2024; Revised: 14 November, 2024; Accepted: 22 November, 2024
Available online: 22 November, 2024 at www.atlas-journal.org, doi:10.22545/2024/00265

Abstract: *Thermal Wave Interferometry (TWI) technique was used to access the thermal diffusivity and thermal conductivity of soils with sandy and clayey textures from Paraná land, specifically from horizons HA (5 to 25 cm) and HB (25 to 76 cm). Experimental setup involved focusing white light on soil samples in titanium wells (100-1200 μm thick), modulated at frequencies from 0.6 to 45 Hz. Results showed that sandy soils had higher thermal diffusivity and conductivity than clayey soils. Open Photoacoustic Cell (OPC) also measured the thermal diffusivity, while TWI determined thermal conductivity ranged from 0.3 to 1 $Wm^{-1}K^{-1}$, and thermal diffusivity from 1 to 9 x 10^{-7} m^2/s. Specific heat was measured using Non-Adiabatic Thermal Relaxation Calorimetry (NATRAC), revealing values between 820 to 920 J/kg·K for HA soils and 940 to 1140 J/kg·K for HB soils. Gravimetric measurements provided soil particle and bulk density data.*

Keywords: Horizons. Lands. Thermal Properties. Thermal Waves.

1 Introduction

Extensive use of soils requires a comprehensive understanding of their physical, chemical, and biological properties [1, 2]. In the civil construction sector, more resistant soils are more adequate to be used as raw material. The sensing of thermal comfort comes from the thermal effusivity (e_s) contact of the materials with the environment. Gas and oil exploration often comes from the examination of soils by specialized professionals who use high-tech equipment to analyze samples

collected from the seabed [3]. The soil itself represents a complex and dynamic system that can overcame many modifications under environmental condition [4, 5]. Therefore, it very important to our knowledge the studies related to soils quality for growing crops, water retain, and mainly properties that can influence soils under pollution. Thus, environmental interventions always come to improve the sustainability and wellness of the earth resources, good and healthy crops depend on it actions [6]. Modified concrete with doping material [7] can be used seeking mechanical properties of soil when applied to concrete molding, prop wall or asphalt pavement, and some engineering are interested in better earth leveling works and draining water, for example.

Nowadays, remote sensing technical instructions are being studied by researchers and scientists of the soils because the spectral response can be found with agility and without causing damage to the environment. Remote Sensing is based on fact that soils present different absorption and reflection with the wavelength according to their physical chemical attributes [8]. Thermal regime of soils is governed by the heating of the surface from solar radiation and the transfer of heat into the interior of the soil through conduction. During the day, the surface warms up, creating a heat flow into the interior. At night, the surface cools by emitting terrestrial radiation (long-wave radiation), causing the reversal of the heat flow direction, moving from the Earth's interior to the surface. Changes in soil temperature throughout the day (temporal variations) and over depth (spatial variations) are studied using horizontal profiles [9]. Heat flux in the soil is basically dependent on its thermal conductivity (k_o), specific heat (c_{ps}), thermal effusivity ($e_s = k_s/\sqrt{\alpha_s}$), and the thermal diffusivity (α_s). Liu *et al*. studied the influence of temperature variation in nitrification of heterotrophic and autotrophic soils [10]. Carbon content, stability of aggregates and main characteristics of humic substances [11] and microbial activity [12] are more affected by varying the temperature in each soil.

Soil classes are taxonomically individualized, classified by their texture, structure and organic matter content. Sandy soils tend to have higher daily temperature amplitudes in the superficial layers and smaller in depth. This is due to the sandy soils have a higher porosity with less contact between soil particles, thus hindering the driving process. In turn, clay soils have more efficiency in conducting heat, having a lower daily thermal amplitude. Thermophysical properties of soil, such as thermal conductivity, thermal diffusivity and thermal effusivity, play an important role in the sustainability of ecosystems and the management of natural resources, because mapping thermal behavior helps in the development of agricultural practices, conservation and soil efficiency [13, 14]. For example, choosing suitable crops for different soil types and implementing conservation techniques such as ground cover and efficient supervision can be adjusted based on the thermal properties of the soil. Thermophysical properties of soil influence the response of ecosystems to climate change. Soils that better regulate temperature and humidity can help mitigate the effects of extreme climate variations, promoting the resilience of natural and agricultural systems [15].

Wang and Zhang [16] observed that soils with higher thermal effusivity generally have good water retention capacity and a denser texture, also, can help moderate temperature variations, promoting a more stable environment for plant growth and microbial activity. Thermal effusivity is particularly important for conserving soil moisture and reducing thermal stress in plants during periods of intense heat.

The main objective of this work is characterized by following thermal properties: thermal diffusivity(α_s), thermal conductivity (k_s) and thermal effusivity (e_s) of the soils with sandy textured (orders Red Argisol and Quarzarenic Neosol) and clayey (Red Latosol and Red Nitosol) from State Parana in Brazil, collected in the surface horizons HA (from 5 to 25 cm) and subsurface HB (from 25 to 76 cm) by means of the Thermal Wave Interferometry (TWI). Thermal diffusivity of Red Argisol samples were also measured by acoustic waves detection using the Open Photoacoustic Cell (OPC). Beyond photothermal and photoacoustic experiments, specific heat (c_{ps}) was obtained by the technique of Non-Adiabatic Thermal Calorimetric (NATRAC), and bulk (ρ_{bulk}) and particle (ρ_s) densities were measured according to the NBR 6508/1984 determined by Brazilian Standard. Results showed how thermophysical properties are dependent on texture and depth in tropical soils.

2 Methodology

2.1 Soils recognition

The study area was concentrated in the State of Paraná, 24˚36` 0` South latitude, 51˚ 23` 0` west longitude, located in Brazilian territory. The state presents a humid tropical climate, temperate climate and wide vegetation, with fifty percent of its territory located at an altitude above 600m and only 3 % at an altitude below 300m. The geology of the state covers a region of transitional zone of basaltic and igneous formation.

This association of geological aspects with characteristics variables and different constituents originating from the intemperance process, being the Red Latosol and Red Argisol as predominating classes, followed by Red Nitossolo, Haplic Cambisol and Quartzarenic Neosol [17]. Figure1 presents the location of soils extraction in Paraná State of Brazil.

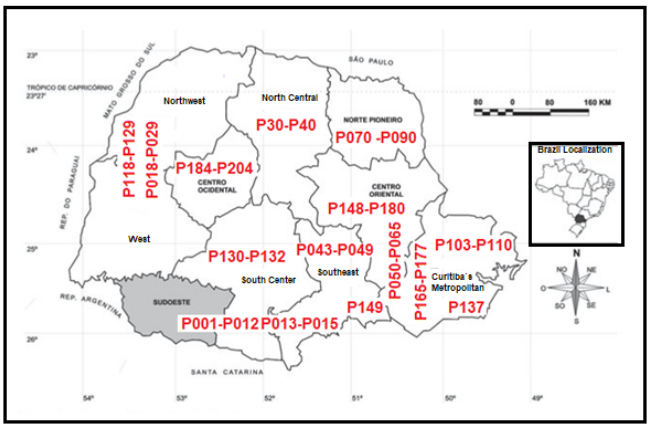

Figure 1: Regions of Parana State where soils were extracted for thermophysical analysis using photothermal methods.

For soil samples storage, collection and georeferencing of the studied sites were utilized specific materials and equipment, among which emphasize: Treaty Dutch type for collecting soil samples at the two studied depths of HA horizons (depths between 5 and 25 cm), HB horizons (depths between 25 and 76 cm), plastic bags and other materials used for packaging, notebooks to register and receive GPS brand Trimble (model GeoExplorer 3) with differential correction for georeferencing points in the field, photographic camera to visual documentation of work area images. Previously the collect, Cezar and coworkers [18] conducted previous studies supported by geographic information system (SIG) with a logistical purpose for optimizing sampling. Sampling density was one point in each 250.000m^2. The collected samples were sent to the Fertility Laboratory of Agronomy Department of the Universidade Estadual de Maringá where they were air-dried and sifted in mesh of 2mm to obtain Dry Earth in the Air (TFSA).

Following the routine physical-chemical analysis described by Cezar et al. [18], the samples were used to identify soil classes. All the material was first dried and then subjected to manual shredding. Chemical treatment was done through the addition of 12.5 % sodium hypochlorite for taking off organic matter and NaOH was used for extraction of sand, silt and clay levels. The sand fraction was segregated by sieving at 53μm of diameter, and the clay fraction was segregated after sedimentation of the silt fraction according to the Stoke's law. Next separation the clay fraction was flocculated by $MgCl_2$ and overage mineral salts were removed by successive washes. In following the clay was dried in an over at 50 ºC for 48 h and next the clay granules were hermetically homogeneous in the mortar. The hardest samples were processed using a Mimoso-brand machine for medium disruption and homogenization. The pulverized raw material was initially sun-dried and then placed in a greenhouse at 60°C for 24 hours to remove excess moisture. Fine blending was done in the mortar with help of the pistil (Soils Laboratory LECIV/CCT/UENF). The remaining powder in each layer, was collected in sufficient amount to carry out the tests (granulometric analysis, liquidity limit, plasticity limit). Levels organic carbon and Fe_2O_3 were obtained according to Brazilian Agricultural Research Company (EMBRAPA) standards.

Table 1 shows granulometry analysis of the samples. Among the studied samples, forty-one samples are Red Latosols (RL) and Yellowy Red Latosols (YL), twenty-one belong to the class of the Red Argisol (RA), twelve of the Haplic Cambisols (HC), ten extracted samples are Quartzarenic Neosols (QN) and two samples are of the class Red Nitosol (RN). Four samples studied classes in this work represent 70 % of the pedological territory of the state of Paraná / Brazil. Its clayey nature, silty and sandy depend on the predominance of the diameter of its grains. The clayey soils are those that present in their composition the predominance of clay above 35 %, and very clayey when a concentration of clayey grains is higher than 60%. To be considered as sandy soil, the sand composition must be higher than 70%, to be conceptualized as medium sandy soil, the soil must be formed between 15% and 70% of sand grains, and finally, silty soils are those that have at least 70% of silts grains.

Samples Identification	**Classification**		**%**				**Predominant Texture**
Code	**Suborder**	**Horizontal Layer**	**Thick Sand**	**Thin Sand**	**Silt**	**Clay**	
391P141	RA	HA	60	04	07	29	very sandy

439P054	RA	HA	56	11	04	29	very sandy
450P097	RA	HA	52	03	42	03	very sandy
458P061	RA	HA	66	02	21	11	very sandy
466P198	RA	HA	66	09	06	19	sandy
620P074	RA	HA	46	25	02	27	sandy
633P072	RA	HA	74	13	02	11	Sandy
523P086	RA	HA	30	48	02	20	Sandy
512P152	RA	HA	36	27	03	34	very sandy
616P084	RA	HA	32	16	27	25	very sandy
511P190	RA	HA	31	30	06	33	very sandy
613P076	RA	HA	21	31	13	35	very sandy
402P097	RA	HB	52	03	03	42	very sandy
422P141	RA	HB	51	04	04	41	very sandy
436P095	RA	HB	57	04	03	36	very sandy
441P059	RA	HB	65	17	02	16	Sandy
624P071	RA	HB	51	18	04	27	very sandy
496P198	RA	HB	44	13	10	33	very sandy
507P211	RA	HB	31	30	04	35	very sandy
424P056	HC	HA	48	16	05	31	very sandy
430P148	HC	HA	19	27	05	49	Clay
443P162	HC	HA	27	06	10	57	Clay
445P055	HC	HA	21	35	05	39	Clay
455P099	HC	HA	49	07	04	40	Clay
615P164	HC	HÁ	19	17	03	61	very clay
429P159	HC	HB	41	06	15	38	Clay
437P099	HC	HB	49	06	04	41	Clay
448P055	HC	HB	15	40	03	42	Clay
476P166	HC	HB	27	22	16	35	Clay
510P152	HC	HB	19	30	04	47	Clay
514P065	HC	HB	11	10	13	66	very clay
401P138	QN	HA	32	31	02	35	Clay
621P075	QN	HA	37	23	02	38	Clay
622P078	QN	HA	24	20	03	53	Clay
442P188	QN	HA	40	18	05	37	Clay
444P151	QN	HA	37	06	10	47	Clay
402P135	QN	HA	35	17	08	40	Clay
421P187	YL	HA	15	10	10	65	very clay
504P079	YL	HA	11	16	03	70	very clay
508P089	YL	HA	23	08	03	66	very clay
449P180	QN	HA	45	11	05	39	Clay
491P183	YL	HA	11	11	09	69	very clay
610P068	YL	HA	21	13	02	64	very clay
483P166	YL	HÁ	21	13	02	64	very clay
604P82	QN	HA	22	16	24	38	Clay
628P080	QN	HA	32	17	16	35	Clay
444P151	QN	HA	37	06	10	47	Clay
510P152	QN	HA	34	27	03	36	Clay
417P060	YL	HA	12	18	02	68	very clay
TAMARANA	QN	HA					
TAMARANA	QN	HA					
TAMARANA	QN	HA					
TAMARANA	QN	HA					
396P138	QN	HB	50	06	04	40	Clay
397P136	QN	HB	25	06	18	51	Clay
412P051	YL	HB	15	07	02	76	very clay
418P189	QN	HB	44	16	04	36	Clay

451P096	QN	HB	46	06	03	45	Clay
489P068	QN	HB	42	13	04	41	Clay
495P210	QN	HB	44	15	06	35	Clay
513P090	YL	HB	13	04	08	75	very clay
525P88	YL	HB	13	15	02	70	very clay
612P33	YL	HB	11	07	04	78	very clay
393P188	QN	HB	40	12	05	43	Clay
394P185	QN	HB	26	09	30	35	Clay
406P180	QN	HB	31	22	03	44	Clay
490P179	QN	HB	13	22	09	56	Clay
399P135	YL	HB	24	11	04	61	very clay
408P136	QN	HB	25	06	18	51	Clay
519P089	QN	HB	26	27	04	43	Clay
518P183	YL	HB	15	18	02	65	very clay
619P180	YL	HB	20	07	12	61	very clay
486P035	RN	HA	11	08	11	70	very clay
486P035	RN	HB	11	08	11	70	very clay
503P066	RQ	HA	72	12	02	14	Sandy
309P139	RQ	HÁ	64	17	04	15	Sandy
413P094	RQ	HA	73	11	01	15	Sandy
600P070	RQ	HA	49	06	12	33	very sandy
411P139	RQ	HB	65	13	03	19	Sandy
475P060	RQ	HB	70	08	03	19	Sandy
454P094	RQ	HB	64	15	02	19	Sandy
414P093	RQ	HB	69	07	05	19	Sandy
607P070	RQ	HB	51	01	03	45	very sandy
494095	RQ	HB	09	08	03	80	very clay

*Mineral soil, composed mainly of organic materials.

***Table 1*:** Particle size analysis of Paraná soil samples.

After that, the soil samples were macerated in the agate mortar for that a large part of the larger agglomerates and grains were fragmented and sieved in 45 μm about 20 minutes. This work was needed due to mathematical photothermal models require better flatness and homogeneity of the material, in addition to reducing the effects of humidity and roughness. Since soil samples were porous, with irregular granules of different sizes, such special care was required. Soil samples were stored in closed acrylic pots to minimize the exchange humidity with the environment. Hematite (α-Fe_2O_3) and sandy samples were also sieved and macerated to prepare them for calorimetric and gravimetric measurements.

2.2 Mapping soil thermophysical properties by thermal wave technique

Thermal Waves Interferometry (TWI) is a remote and nondestructive technique used to thermophysical characterization of solids and gases and to detect defects in layers and coatings. Bennet and Patty`s model [19] foresees that while solid surface is excited with modulated and focused light, thermal waves are generated in the material. These waves propagate by means of thermal conduction to substrate-sample and sample-gas interfaces, where they are reflected successively until they are completely attenuated by e^{-x/μ_s}, in which $\mu_s = \sqrt{\frac{2\alpha_s}{\omega}}$ is known as the sample's thermal diffusion length, α_s, is the thermal diffusivity, and ω is the light modulation angular frequency. The main effect of the reflection of thermal waves in the sample is the fluctuation of the surface temperature, θ. The surface temperature oscillation is a complex quantity mathematically depicted by the integration of the sum of the reflection's contributions at the interfaces in the whole sample thickness, l_s. Equation (1) shows that temperature fluctuation behaves faultlessly as an evanescent space wave, decreasing exponentially to points distant from heat sources.

$$\theta = \frac{I_o \beta T_g}{4k_s\sigma_s(1 - R_b R_g e^{-2\sigma_s l_s})}\left[\frac{1 - e^{-(\beta+\sigma_s)l_s})}{\beta + \sigma_s} + \frac{R_b e^{-2\sigma_s l_s}}{\beta - \sigma_s}(1 - e^{-(\beta-\sigma_s)l_s})\right]. \quad (Equation\ 1)$$

In which, I_o, is the light beam initial intensity, β is the opacity coefficient of sample, $\sigma_s = \frac{(1+i)}{\mu_s}$, is the complex sample thermal diffusion coefficient, $R_b = \frac{e_s - e_b}{e_s + e_b}$, $R_{bg} = \frac{e_s - e_g}{e_s + e_g} \sim 1$, are respectively the reflection coefficients at the substrate-sample and sample-gas interfaces, associated to the thermal effusivity of the sample, e_s, substrate, e_b, and gas, e_g, respectively, and, $T_g = \frac{e_s}{e_s + e_g}$, is defined as the transmission coefficient of the sample for the gas [20]. Considering that the opaque sample is normalized by thermal thickness, $\frac{l_s}{\mu_s}$, phase shift, φ, between a reference and samples and is set by:

$$\varphi = \tan^{-1}\left\{\frac{R_b(1 + R_g)e^{-2\frac{l_s}{\mu_s}}\sin(2\frac{l_s}{\mu_s})}{1 - R_g\left(R_b e^{-2\frac{l_s}{\mu_s}}\right)^2 + R_b(1 - R_g)\cos(2\frac{l_s}{\mu_s})}\right\}. \quad (Equation\ 2)$$

Phase shift is independent of the magnitude of the absorbed and reflecting energy in the surface. Phase shifts are influenced by the material thickness due to the super damped and harmonic nature of thermal waves. In practice, measurements are taken over a wide frequency range, which

influences the depth of heat penetration of the thermal wave in the sample until reaching $\varphi \cong 0$, finding the thermally thick regime of the wave. The exchange between the thermally thin and thick regimes thermal wave are observed at the points of inflection of the curves, that is at, $\frac{l_s}{\mu_s} = 0.75$ for signal amplitude, and $\frac{l_s}{\mu_s} = 1.5$ to phase [19]. Simulation of Eq. (2) is shown in Figure 2 using several values of R_b from Rb=-1(shift ~ +45) to Rb=+1(shift ~ -45).

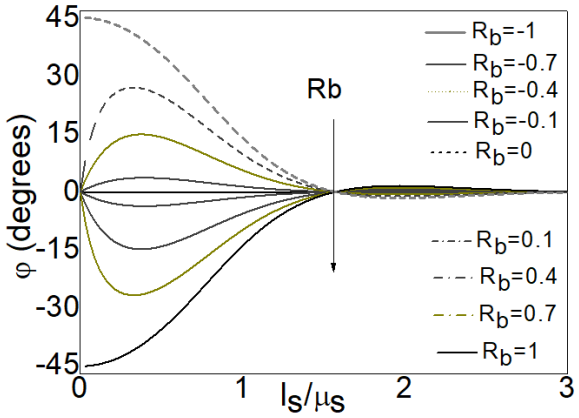

Figure 2: Normalized phase shift thermal wave of the opaque sample in range $-1 \leq R_b \leq 1$.

TWI setup is presented in Figure 3. The system consists of a Xenon arc lamp emitting white light (Oriel Instruments, model 68820), a chopper (Stanford Research Systems, model 540) modulating the light, a thermopile (Oriel Instruments, model71755) with a Germanium (Ge) window with transmission in 90 % at range (8-14) μm to read the sample average surface temperature fluctuation, a lock-in amplifier (Stanford Research Systems, model850) which uncouple phase and amplitude signal monitored with the thermopile at the reference frequency of the chopper, and a X-Y stage driven by a bipolar stepper motor (API GETTYS, model 230-6102BN) accurately 10 steps/mm and course of 10 cm for the X-Y stage, limited by two path final sensors (PAI 0221) operating in the clockwise and counterclockwise directions. A computer with an acquisition program was employed to receive, update and store the preamplifier data, communicate with the power supply of the step motor and control the voltage received by path final sensors. Two flat-convex lenses BK7 with focal length $f`$ of 10 and 15 cm, a flat mirror and a flat-convex lens BK7, $f`$ = 5 cm were used to collimate light beam and helping to focus the light on the sample. Scheme is shown in Figure 3a.

Samples already macerated and sieved were placed with the aid of a spatula in wells of varying thicknesses, between 100 to 1200 μm, onto a titanium (Ti) substrate machined with the thickness $l_b = 2$ mm. As shown in Figure 3b, the soil was deposited in the wells and smoothed by a blade to ensure flatness of the surface in the desired thickness. Substrate was put on the X-Y stage moving from 0 to 100 mm while the sample's face and of the substrate illuminated by a fixed light modulation frequency, f.

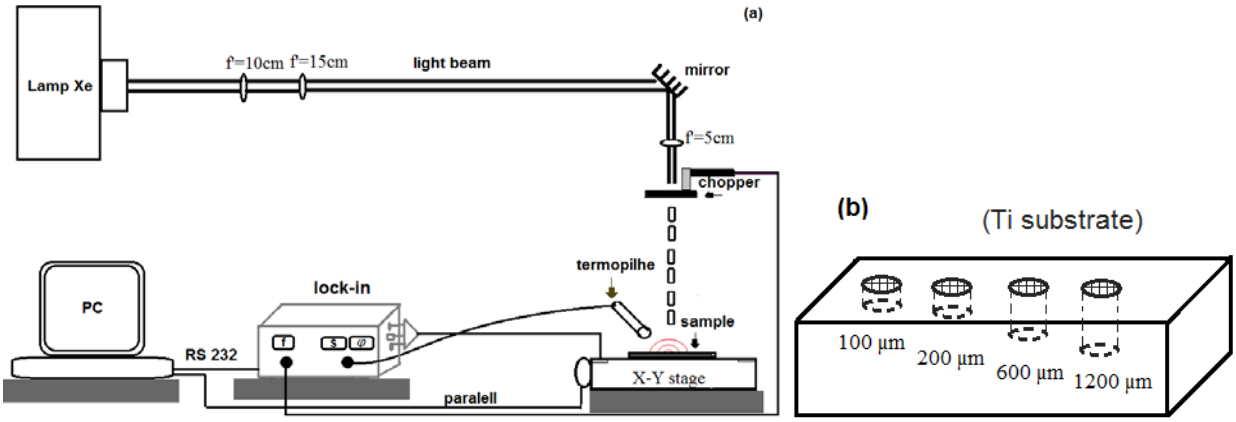

Figure 3a: TWI experimental setup and **Figure 3b:** Soil samples put titanium substrate.

During the experiment, the thermopile monitored the surface temperature fluctuations of both the substrate and the sample at regular intervals of 0.5 mm (five steps). The procedure involved taking an average of 10 readings per point, with measurements performed at twice the time constant of the lock-in amplifier, t=3s, updating the position during acquisition. These data were recorded in tables per position, signal and phase, and then plotted in graphs (signal vs. position and phase vs. position). Measurements were repeated within the frequency range of 0.6 to 45 Hz. The wells in which each sample was deposited had a diameter of 6 mm and were spaced 10 mm apart on the substrate. During laboratory tests, the ambient temperature was adjusted to 25°C, and the relative humidity of the air was monitored using a thermo-hygrometer (ICEL Manaus, model HT-4000). The samples were measured again after being dried in a greenhouse for 24 hours (FANEM LTDA, model 311 CG) at approximately 105°C. Thermophysical properties of the soils measured immediately were: thermal diffusivity (α_s), thermal effusivity (e_s), and indirectly thermal conductivity (k_s).

2.3 Thermal diffusivity investigation by photoacoustic method
2.3.1 Samples preparation

To prevent soil compaction and ensure uniform sample dimensions, sample holders were made from 12 µm thick aluminum foil, used as layers for thermal coupling due to its ease of acquisition and handling. In this setup, the coefficient of thermal diffusion is greater than the thickness of the metal sheets ($\mu_0 > l_0$), given that the cutting frequency of aluminum is around 7 kHz. Consequently, for measurements up to 220 Hz, the aluminum layers are considered thermally thin. Figure 4 illustrates the sample holders used for storing soils. A vacuum grease was employed to seal each sample holder. A total of twelve samples were prepared, with two samples of each class extracted from horizons HA and HB. Each sample had a diameter of 10 mm and a thickness ranging from 221 to 284 µm.

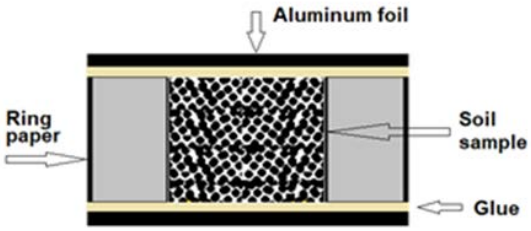

Figure 4: Soil's sample support.

2.3.2 Thermal diffusivity

Experimental setup used for measuring thermal diffusivity is shown in Figure 5.

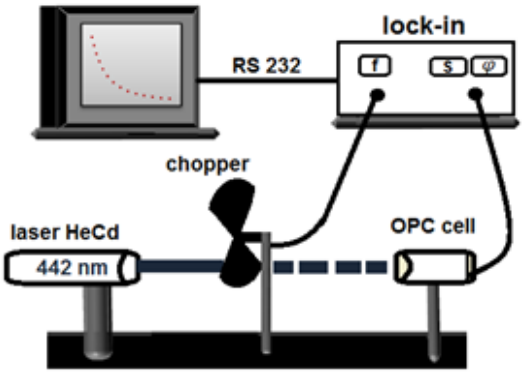

Figure 5: Experimental OPC setup for thermal diffusivity measurement of soils.

Vacuum grease was used to seal the sample in the cell. A modulated light beam was directed at the back of the sample, causing heat to diffuse through the material until it reached the other side. A He-Cd laser (K Series, KR KiMMON, model IK5652R-G) with a power of 120 mW at 442 nm was used as the excitation source, modulated at frequencies ranging from 10 to 220 Hz. As the samples heated due to the absorption of modulated light, pressure oscillations within the cell, matching the frequency of the chopper, were detected by an electret microphone (model WM-61A, Panasonic) in the cell's OPC. The signals were recorded by a lock-in amplifier in terms of phase and amplitude, with values stored on a microcomputer. According to the model proposed by Rosencwaig and Gersho [21], considering thermal diffusion as the primary mechanism for generating the photoacoustic signal, the equation governing the pressure fluctuations in the air chamber is described by:

$$\partial P = \frac{\gamma P I_o}{2\pi l_g k_s f\, \theta_{amb} \sinh(l_s \sigma_s)} \sqrt{\alpha_s \alpha_g}\, e^{i(\omega t - \frac{\pi}{2})}. \quad (Equation\ 3)$$

In Eq. (3), P is the ambient pressure, α_s is the surrounding gas thermal diffusivity and ls is the gas thickness. Photoacoustic signal corresponds to the non-temporal part of the pressure fluctuation ∂P. Thermal diffusivity can be calculated according to the thermal regime that sample

is found. In thermally thin regime (sinh(x)~x), pressure fluctuation is proportional to $f^{-3/2}$, like is represented by Equation. (4)

$$\partial P = \frac{\gamma P I_o}{(2\pi)^{3/2} l_g l_s k_s f\ \theta_{amb}\ f^{3/2}} \sqrt{\alpha_g \alpha_s}\ e^{i(\omega t - \frac{3\pi}{4})}. \ (Equation\ 4)$$

On the other hand, in frequencies above the critical frequency, (f_c), the sample is termed as thermally thick and the equation follows the approximation sinh(x)~e^{-x}, then, $\partial P \approx \frac{e^{-b\sqrt{f}}}{f}$:

$$\partial P = \frac{\gamma P I_o}{(2\pi)^{3/2} l_g l_s k_s f\ \theta_{amb}\ f^{3/2}} \sqrt{\alpha_g \alpha_s}\ e^{i(\omega t - \frac{\pi}{2} - \frac{l_s}{\mu_s})} \frac{e^{-b\sqrt{f}}}{f}. \ (Equation\ 5)$$

In which, the constant b is given by $b = l_s\sqrt{\frac{\pi}{\alpha_s}}$. Photoacoustic signal amplitude for a sample terminally thick decrease exponentially [22] with the modulation frequency, i.e., $S_{PA} \propto \frac{e^{-b\sqrt{f}}}{f}$. In OPC, α_s is obtained from the adjustment of experimental results from coefficient (b) in exponential argument (-b $\sqrt{f}$). The cut frequency found for the soils was around 7 Hz, i.e., as all the measurements in this work are comprised from 10 to 220 Hz, the thermally thick regime was guaranteed.

2.4 Specific heat measurement: thermal relaxation calorimetry at ambient temperature

Thermal relaxation calorimetry is a technique that measures temperature fluctuations as a function of time following the application of a heat pulse [23]. A detailed description of this theory is presented by Barucci *et al*. [24].

In the tests, the initially empty substrate was heated by a laser beam during 60s until temperature of 25°C. Soon after, the beam light was interrupted by a shutter and the heat was dissipated by a silver substrate during the same time interval of the heating cycle. Temperature variation between the thermal reservoir and the substrate was read by a thermocouple K-type coupled to the substrate and connected to a nano-voltmeter (Keithley, model 2182) which measured the potential difference related to the temperature difference as a function of time transmitting the data to a computer. Temperature monitoring of thermal reservoir was performed by a temperature controller (LakeShore, model 340).

Forthwith, an aluminum substrate of known mass (24.5 mg) was fixed on the silver substrate and the measurements of heating and thermal relaxation cycles were retrying, so that power absorbed by the system was 20mW. Tests shown that the fused silica specific heat experimentally found was equivalent to (734 ± 5) $J.Kg^{-1}.K^{-1}$, exhibiting a relative percentage error lower than 0.2% to the literature. After calibration, approximately 12 mg of the soil samples, shown in Table 2, and sand and hematite samples were measured by NATRAC. All measurements masses were made on digital scale balance (AND, model GH202-50 μg precision).

2.5 Bulk density and particle density

Soil density can be understood in two ways: bulk (ρ_{sbulk}) and particle (ρ_{spart}). Bulk density is defined as the ratio of the dry soil mass (m_{ss}) in the greenhouse after 24 hours drying at least, 105 °C, per volume (V_t) filled by the soil in a recipient including solid and porous fraction:

$$\rho_{s\ bulk} = \frac{m_{ss}}{V_t}. (Equation\ 6)$$

Particle density is equivalent to the density of the soil based on the volume of the solid fraction. The particle density was determined by measuring the amount of ethyl alcohol required to fill the pipette to 25 ml, and the results were calculated accordingly.

$$\rho_{s\ part} = \frac{m_{ss}}{V_l}\ \rho_l. (Equation\ 7)$$

In which, ρ_l = 789 Kg. m^{-3} is the ethyl alcohol density.

About 10g of the soil samples and sandy were weighed and taken to the greenhouse (FANEM LTDA, model 311 CG) to dry at temperature 105°C. The samples were again weighed, and their masses recorded. Gravimetric humidity was calculated according to the NBR 6508. Following that, the samples were put in the volumetric pipette with the helpfulness of a funnel and bulk density was compute by Eq. (6). Soils specific mass was determined through addition of hydrated ethyl alcohol 92.8°ppm grade putting slowly until it reaches the mark of 25 ml in the meniscus of the pipette. The liquid volume (V_l) was transferred to another pipette and the soil particle density was calculated by Eq. (7).

3 Results and Discussion

3.1 Thermophysical properties mapping by thermal wave technique

Although photothermal techniques are well-known and applied in the characterizations of the natural porous materials, as hydroxyapatite [18, 25, 26], analytical methods for soil recognition, as carbon content and minerals, are very efficient [27-31], and effects with addition of elements in the soil already analyzed, for example, addition of selenide in soil adsorption to either increase its fertility [32], the actual work is a pioneer in the characterization and thermal mapping of Brazilian tropical soils by Thermal Waves Interferometry technique. The 85 samples were measured and characterized by TWI, as shown in Table 1. Among photothermal techniques, TWI presents some advantages to assess thermophysical properties of the soils: samples do not have to be compacted, readings are done in real time, technique has good suitability for porous and heterogeneous materials, thermal analyzes are fast and important properties can be determined [33, 34].

Initially, the signals and phases of the samples were recorded during the frequency scans. It was observed that, starting from 15 Hz, the phase difference among all thicknesses was completely damped. Next, average phase (φ) were plotted as a function of normalized thickness with frequency $l_s\sqrt{f}$. Characteristic curve of the normalized phase at the highest modulation frequency observed in the measurements is presented. For a more comparative approach, consider the phases obtained at a 3 Hz frequency for samples RL393P188HB, QN454P039HB, and RL444P151HA,

respectively, presented in Figure 6. Measured phase varies from sample to sample based on their characteristics.

The dashed line indicates a measurement on the substrate. Black lines drawn on plateaus represent the average phase found at the respective sample thicknesses measured at a fixed frequency. Soil porosity causes the phases to fluctuate on the plateau because the measurement is made on the irregular grains of the soil along a 6 mm extension of each sample thickness.

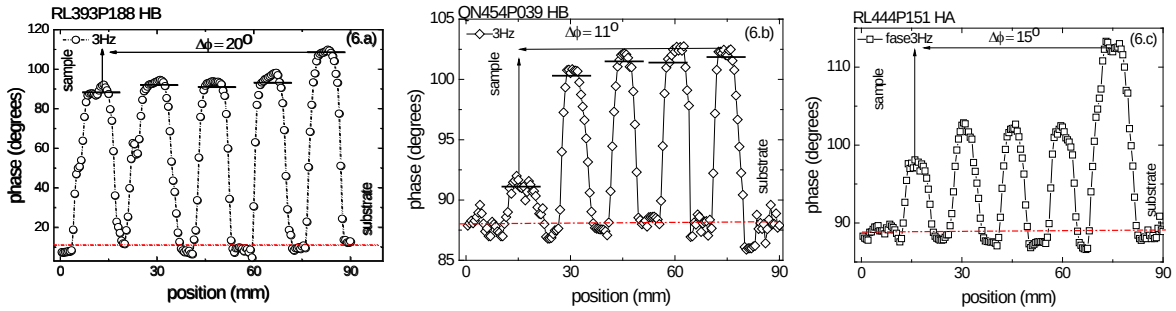

Figure 6a: Experimental phase shift data obtained for soil RL393P188HB; Fig. **6b:** for QN454P039HB, and Fig. **6c:** for soil RL444P151HA. All experiments used laser scanning on samples.

The determination of thermal diffusivity and reflection coefficient were obtained from the characteristic curves of the normalized wave lag by thicknesses of scans over a wide frequencies range. Fittings are made using the Eq. (2). Some characteristic curves are displayed in Figures 7a, 7b and 7c to the samples LE393P188HB, RQ454P039HB and LE444P151HA, which showed phase shifts of 19º, 11º and 11 º, respectively, with the reflection coefficient, R_b = - (0.50 ± 0.02), R_b = - (0.29 ± 0.02), and R_b = - (0.30 ± 0.02).

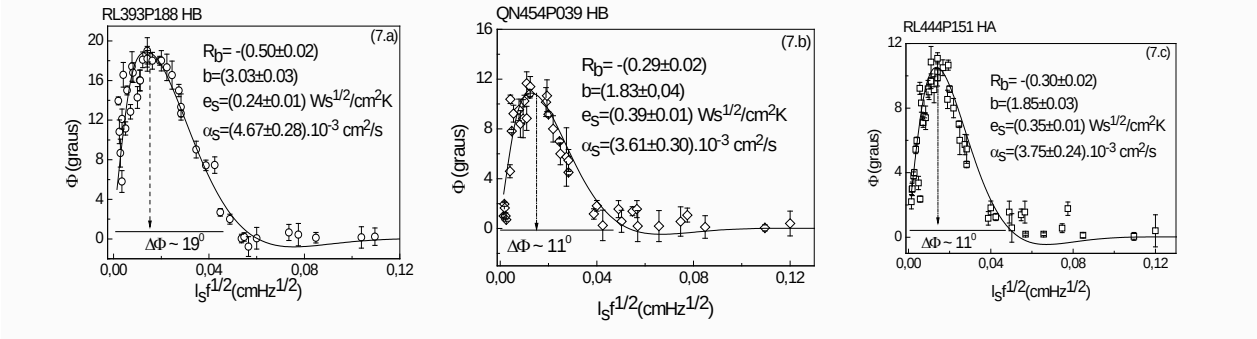

Figure 7: Fitting of the data using Eq. (2) of soils Fig. **a:** RL393P188HB; Fig. **b:** QN454P039HB, and **Fig. c:** RL444P151HA, all using the TWI phase shift data.

Negative sign of the coefficients is explained by the fact that the soils are thermally less conductive than the titanium substrate e_b =7172 $W.\sqrt{s}.m^2.K^{-1}$ [20]. Thermal effusivity, e_s, is

calculated by means of the expression $e_s = e_b\left(\frac{1+R_b}{1-R_b}\right)$, and thermal conductivity, $k_s = e_s\sqrt{\alpha_s}$, was also calculated. In the curves shown in Figure 7, the characteristics of the results indicate a more pronounced phase shift and sharper width in the argisol sample extracted from the subsurface horizon. Experimental results from other samples were fitted using the phase shift model of the opaque sample. Results, which describe the average values of the thermophysical properties of studied soil classes and extraction horizons, are shown in Figures 8a, 8b, and 8c.

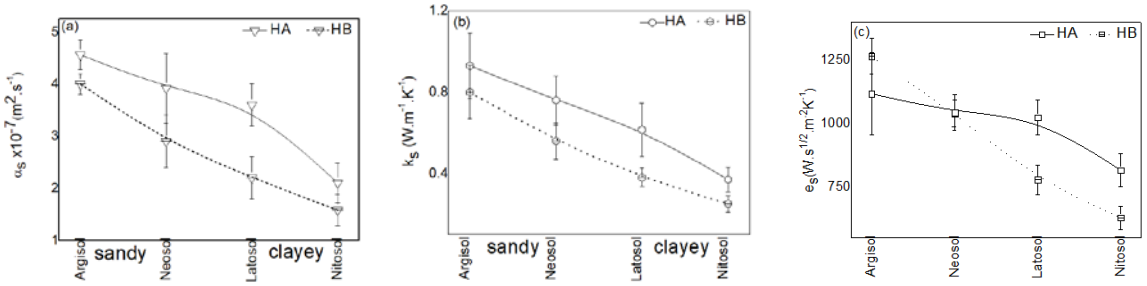

Figure 8a: Group of soils average thermal diffusivity measured by TWI method, one note that slope is decrescent from "sandy" toward "clayey" soils, Fig. **8b:** Soils thermal conductivity and Fig. **8c:** Soils thermal effusivity. Both stratus HA and HB follow a similar behavior for the three thermophysics properties.

Given that each type of soil has specific physicochemical attributes, it is essential to note that thermal properties can be influenced by various factors, such as texture and chemical composition. Results from TWI indicate that the mineral structure affects the thermal diffusivity and thermal conductivity of soil. In sandy soils, around 60% of the mineral composition consists of silicates, whereas in clay soils, at least 35% of the mineral content comprises iron and aluminum oxides. Silicate minerals conduct and diffuse heat more intensely and quickly than ferric oxides. Heat transfer in the surface layers of the soil, resulting from thermal disturbances due to direct solar irradiation and the incorporation of organic matter into the horizon HA, may slightly increase the thermal transport properties of the soil. This is because each studied layer of soil has a specific composition. Deep layers are strongly stratified. Figures 8a and 8b show that the thermal diffusivity was established in the range from 3 to 5 x 10^{-7} $m^2.s^{-1}$ in thick textured soils, and between 1.6 and 3.6 x 10^{-7} $m^2.s^{-1}$ for clay soils, and thermal conductivity was set in the range from 0.56 to 0.93 $W.m^{-1}.K^{-1}$ for the samples at the classes of the Red Argisol and Quarzarenic Neosol, and between 0.25 and 0.46 $W.m^{-1}.K^{-1}$ for soils Red Nitosol and Red Latosol. Thermal diffusivity controls the rate in which the thermal waves propagate through soil layers. The absence of water impedes heat flow in the soil, making it difficult for the topsoil to transfer heat to the lower layers.

Average values of thermal diffusivity are in good agreement with the range reported by other studies that used harmonic and logarithmic models to analyze French soils. Thermal conductivity of soil depends on its structure, moisture, and texture. The granule size in clayey soils is smaller than 2 μm, whereas in clay soils, the diameters can reach up to 50 μm. Smaller diameter soils require more particles to create porosity, which increases the resistance of these particles. In clayey soils, there is good particle contact and improved water storage, which inhibits heat diffusion and affects the heat transfer process.

This phenomenon suggests that sandy soils heat up faster on the surface when exposed to the same irradiation. The increase in k_s with sand content is therefore a consistent result. Results indicate that soil tends to diffuse more heat at the surface and at shallower depths.

Thermal effusivity (Figure 8c) shows the same behavioral tendency of thermal transport properties in relation to soil textures. Soil is a thermal insulation, which directly influences the parameter of heating regulation on the contact surface, that is, thermal effusivity. For the Parana soils, the thermal effusivity remained determined within the limits of 630 until 1300 $W.\sqrt{s}.m^{-2}.K^{-1}$. Due to its low thermal effusivity, the soil can retain heat for a longer period, which contributes to slower surface temperature fluctuations. This helps to mitigate the effects of sudden changes caused by climate variation, and daily cycles to which soils are constantly exposed. Soils have a hydrophilic nature due to their mineral composition and aqueous fraction. Experiments demonstrated that the gravimetric moisture, which represents the minimum soil moisture after drying processes in the greenhouse, was lower than 6% in all measurements.

Soil temperature is strongly influenced by its thermophysical parameters. To opaques samples ($\beta l_s \gg 1$) the superficial temperature equation, Eq. (1), can be simplified by being rewritten as:

$$\theta = \frac{I_o}{2k_s\sigma_s}\left[\frac{1 + R_b e^{-2l_s\sigma_s}}{1 - R_b R_g e^{-2l_s\sigma_s}}\right]. (Equation\ 8)$$

By adopting a thickness of 100 μm and a frequency of 3 Hz, the electromagnetic wave intensity reaching the sample (2 W) was measured using a power sensor. Thermal conductivity and thermal diffusivity obtained from thermal wave analysis are presented in Table 2, which shows the real part of the heating for the following samples. The heating in the samples exceeded 2 Kelvins in clay soils and was less than 1.7 Kelvins in sandy soils. Experiments did not show significant temperature changes at different soil depths.

Sample	$R_b \pm \Delta R_b$	$\alpha_s \pm \Delta\alpha_s$ (10^{-7} $m^{-2}.s^{-1}$)	$k_s \pm \Delta k_s$ (10^{-1} $W.m^{-1}.K^{-1}$)	$\theta \pm \Delta\theta$ (K)
RN486P035-HA	$-(0.64 \pm 0.04)$	1.56 ± 0.33	6.31 ± 0.15	2.04 ± 0.10
YL508P089-HA	$-(0.64 \pm 0.03)$	1.55 ± 0.16	6.37 ± 0.09	2.01 ± 0.11
RA620P074-HA	$-(0.52 \pm 0.03)$	2.16 ± 0.34	10.47 ± 0.23	1.44 ± 0.09
RQ413P084-HA	$-(0.58 \pm 0.03)$	1.99 ± 0.30	8.61 ± 0.16	1.69 ± 0.10
RN494P035-HB	$-(0.63 \pm 0.03)$	1.31 ± 0.39	5.84 ± 0.13	2.01 ± 0.11
YL525P088-HB	$-(0.69 \pm 0.03)$	1.37 ± 0.40	4.93 ± 0.12	2.44 ± 0.13
RA624P071-HB	$-(0.52 \pm 0.02)$	2.02 ± 0.25	10.19 ± 0.16	1.44 ± 0.10
RQ414P093-HB	$-(0.55 \pm 0.03)$	1.68 ± 0.24	8.48 ± 0.14	1.57 ± 0.09

Table 2: Thermal properties found by means of surface heating.

3.2 Comparison between thermal diffusivity obtained by OPC and TWI for argisols

Twelve dry samples of Argisol extracted from the horizons HA and HB were measured using a Photoacoustic Cell. Figure 9 shows a log-log graph of the Photoacoustic signal magnitude versus

frequency for the Argisol sample 512P212 collected from horizon HB. Thermal diffusivity was determined by fitting the photoacoustic signal with Eq. (5). Table 3 indicates that the thermal diffusivity ranged from 6.5 to 9.5 x 10^{-7} $m^2.s^{-1}$, with approximately 10% relative uncertainty, and no significant behavioral differences between horizons HA and HB. The best fit was found in the frequency interval from 57 to 120 Hz. Above 120 Hz, the linear behavior of the signal was not obtained due to the influence of thermoelastic and photobaric effects.

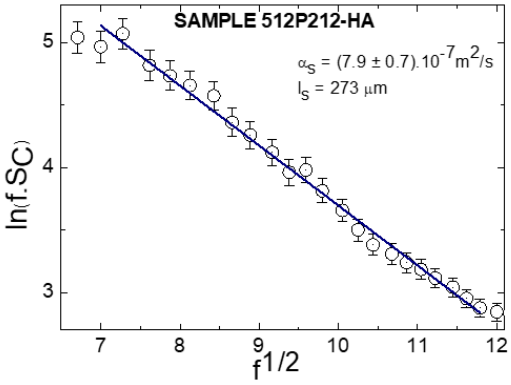

Figure 9: Linear fitting of OPC signal data to Argisol having 273 μm thickness. Sample 512P212HA. Typically, the OPC experiment allows the thermal diffusivity value of soil sample, and for the Argisol, it was found $\alpha_s = 7.9 \pm 0.7$ x 10^{-7} $m^2.s^{-1}$.

Sample Code	Layer Horizontal	$l_{\text{sampleport}}$* μm	l_{glue}* μm	l_s* μm	α_s (10^{-7} x m^2. s^{-1})
439P054	HA	307	36	247	9.4± 0.8
450P097	HA	291	30	237	8.7± 0.6
512P212	HA	320	23	273	7.9± 0.7
523P086	HA	286	20	242	6.7± 0.2
613P076	HA	272	27	221	6.3± 0.4
616P084	HA	282	10	248	6.5± 0.5
410P097	HB	307	27	256	9.2± 0.6
436P095	HB	290	25	241	9.4± 0.8
441P059	HB	282	17	241	7.3± 0.5
516P190	HB	329	21	284	8.1± 0.4
619P080	HB	314	20	270	8.6± 0.7
623P072	HB	313	14	275	8.6 ± 0.7

*Thickness error measured by the micrometer Mitutoyo (MDC-25SB) was 1 μm.

Table 3: Thicknesses of the Argisols sample port and samples prepared for OPC.

Comparing the thermal diffusivity determined by OPC with that obtained by TWI shows that both techniques agree in terms of the order of magnitude for the soils characterized. TWI is more sensitive to measurements in porous media compared to OPC because it minimizes the effects of air flow and pressure fluctuations within the pores. Another advantage of the TWI technique is that its theoretical model for opaque samples is described by non-transient parameters and can be applied over a wide frequency range for thermal wave oscillation. In contrast, the OPC model for thermal diffusion works only within a narrow frequency range and is subject to photobaric and

thermoelastic effects. However, using powdered samples for OPC was an effective method for capturing the photoacoustic signal from the soils [22].

3.3 Specific heat and density

Specific heat was obtained using the non-adiabatic thermal relaxation calorimetry technique, which involves heating and cooling cycles of the samples over time. Figure 10 shows the results of the specific heat measured for the various studied soils. Soils are heterogeneous materials composed of minerals, air, water, and organic matter. According to the de Vries model [35], the specific heat of soils is determined by the sum of the products of each constituent's specific heat and its corresponding volume fraction. Specific heat of water is 4180 $J.Kg^{-1}.K^{-1}$, of air is 1000 $J.Kg^{-1}.K^{-1}$ and that the specific heat known in the literature for hematite, goethite, sandy and silica are c_{pFe2O3} = 670 $J.Kg^{-1}.K^{-1}$, $c_{pgoethite}$ = 800 $J.Kg^{-1}.K^{-1}$, c_{psandy} = 820 $J.Kg^{-1}.K^{-1}$, c_{pSiO2} = 730 $J.Kg^{-1}.K^{-1}$, respectively, and also organic matter [36, 37]. We can observe in the graph that organic matter changes the sensitivity of heat. In the subsurface horizons, more impoverished in organic compounds, the specific heat determined was established in the range from 936 to 1145 $J.Kg^{-1}.K^{-1}$, at the same time as for samples of horizon layer HA, specific heat was between 820 and 927 $J.Kg^{-1}.K^{-1}$.

Experimental measurements of specific heat for hematite and sandy soils showed good agreement with the literature. In horizon HA, the specific heat of the Nitosol and Latosol was slightly higher than that of the Argisol and Nitosol samples. In horizon HB, this increase was in the range of 10 to 20%. Soils are composed of approximately 50% of minerals and organic matter, and 50% of water and air. The higher moisture content in clayey soils, which have a more hydrophilic nature, may have contributed to their increased specific heat. Experimental errors were calculated using the standard deviation in the graph fitting software.

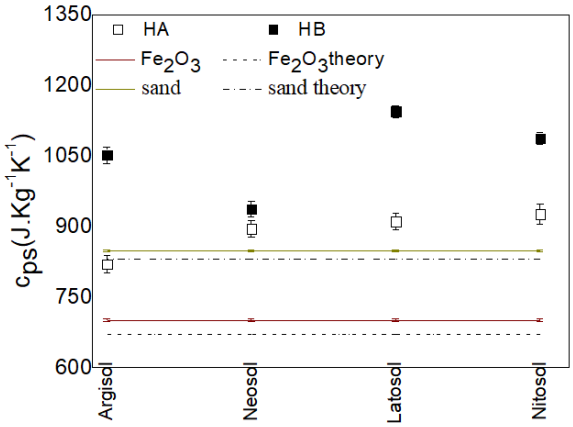

Figure 10: Specific heat of soils of the Parana, this figure also shows the predicted value of "sand" and for "iron oxide" (hematite).

Figures 11a and 11b show the bulk density and particle density of the soils. It is observed that both bulk density and particle density changed slowly with soil depth. Bulk density remained relatively stable at 1350 $Kg.m^{-3}$ to clayey soils, and fluctuated between 1400 and 1900 $Kg.m^{-3}$ to sandy samples, while the particle density was found from (2212 ± 190) $Kg.m^{-3}$ to (2494 ± 221)

Kg. m^{-3} and (2527 ± 216) $Kg.m^{-3}$ to (2723± 262) $Kg.m^{-3}$ in thin and thick textured soils, respectively.

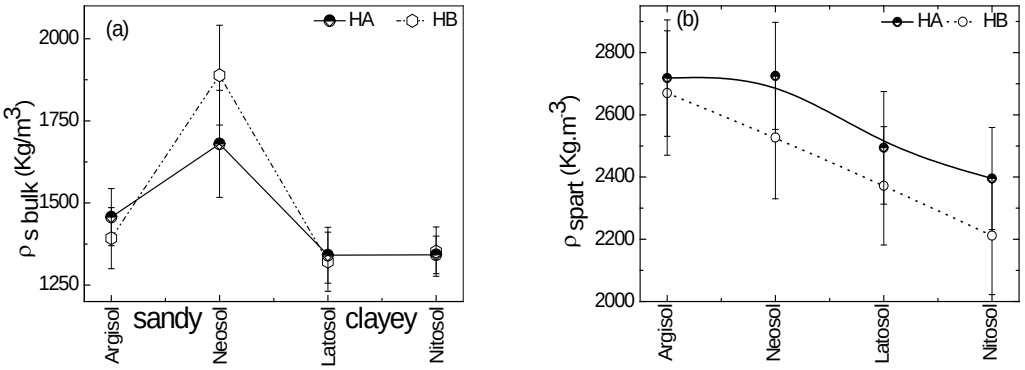

Figure 11a: Soils of Paraná bulk density and Fig. **11b:** Soils Paraná particle density.

Density is associated with the compaction, structure, aggregation of organic matter, and porosity of the samples. Soil density is an important physical attribute for providing information on their conservation status control for infiltration and water retention, root development, gas exchange and susceptibility of this soil to erosion processes. Sand grains are approximately the same size as clay aggregates, but sand grains lack micropores. As a result, coarse-textured soils are denser than fine-textured soils. In clay soils, in addition to the porous space between aggregates, there are internal micropores. This structure provides more distributed porous space throughout the volume, leading to lower soil density. In sandy soils the concentration of organic matter is generally small, solid particles are little predisposed to cohesion and stickiness barring the clusters formation. Organic matter is hugely light weight floating between 200 and 400 $Kg.m^{-3}$ and variable because of its complex composition, being altered by the decomposition time, wastes and residues. We found for natural sand (formed of 97% quartz, and wholly devoid of organic matter) an apparent density equal to 1997 $Kg.m^{-3}$, showing more dense than other soil samples with a sandy texture. While apparent density is based on ratio of mass and volume of dry soil, the bulk density only refers to the measurement of the specific mass of the solid fraction of the soils, while the density of particles is an unchanging property, independent of the dry and saturated soil conditions, the single attribute that significantly interferes in specific mass is the concentration of organic matter.

3.4 Final considerations about thermophysics properties soils

Results reported in literature indicated that the thermophysics properties determined in tests may be influenced by composition and amount organic matter present in soils. Soils from Parana are submitted to the tropical climate. Researches made on American, European, and Brazilian soils showed the properties found are influenced by a factors group, such as, soils in the natural state, dry, with fine and thick textures and extracted at different depths. As an example, Brazil's soils from the "caatinga" region (brushwood vegetation found in the Northeast of Brazil) were studied

and results from Silans [38] reported similar values for the thermal diffusivity of horizons HA (0 to 15cm). This region faces strong dry soils as well as soils interfaces with severe thermal gradient. In the opposite conditions, another reported result is found for the tundra ground in polar region. Such as very wet soils and low temperatures produces small thermal gradient in the soil's stratus. Bodzenta and coworkers [39] found values of thermal diffusivity from 7 to 34 x 10^{-3} cm^2/s for the horizon HA e HB (from 0 to 40 cm deep), with results representing typical properties for a mix soil with gravel, small stones, sand, clay and rocks, and they report the errors about 20% under the severe conditions from summer to winter in those location.

Reported values [27, 28] showed that thermal diffusivity (α_s) and the volumetric thermal capacity ($\rho_s c_{ps}$) from soil mixed with sand with humidity, and with the natural humidity, varying from 9 % to 38 %. Tests confirm that experimental results behaved satisfactorily with the prediction of the De Vries model [35]. Average thermal diffusivity and $\rho_s c_{ps}$ from soils with 9 % natural humidity were 9 x 10^{-7} $m^2.s^{-1}$ and 1.66 x 10^6 $J.m^{-3}.K^{-1}$. After the addition of water to each mm the liquid volume inside the soil slightly modified the behavior of thermal diffusivity and $\rho_s c_{ps}$, characterizing in a reduction of the diffusivity in the range from 9 to 8 x10^{-7} $m^2.s^{-1}$ and an increment of thermal capacity volumetric up to 6.25 x 10^6 $J.m^{-3}.K^{-1}$ · Employing the technique of the dual probe, Bristow and collaborators [28] characterized three American soils: Sandfly (100 % sandy), Clayton (98 % sandy) and Clarinda (clayey) dry, by determining the thermal diffusivity of the sandy soils $\alpha_s = 2.3$ x 10^{-7} $m^2.s^{-1}$ and $\alpha_{s\,(clarinda)} = 1.97$ x 10^{-7} $m^2.s^{-1}$. Soils volumetric thermal capacity was measured for Sandfly and Clayton as 1.2 x 10^6 $J.m^{-3}.K^{-1}$ and 0.9 x 10^6 $J.m^{-3}.K^{-1}$, respectively.

Nicolau and collaborators [40] characterized the thermal conductivity of the Yellow Latosol and the Neosol, using the Campbell model, obtaining, $k_{s\,(nitosol)} = 0.26$ $W.m^{-1}.K^{-1}$, and $k_{s\,(yellow\text{-}argisol)} = 1.44$ $W.m^{-1}.K^{-1}$. Temperature fluctuations and heat flux were monitored in Marajo Island between 2001 and 2005 [41], with the objective of comparing the thermal responses to daily heating. Thermal diffusivity and thermal conductivity were monitored during this period at depth levels, 0.00, 0.25 and 0.50 cm. Mean temperature obtained in the respective depths were, 303.3, 301 and 298 K, and the mean thermal diffusivity in the layers varied between 7.2 and 8 x 10^{-7} $m^2.s^{-1}$ in the dry period, and from 7.9 to 28 x10^{-7} $m^2.s^{-1}$ during the rainy season [42] working with two soils types, classified as sandy and franco. Using the double probe method, the thermal conductivity found varied from 0.98 to 2.17 $W.m^{-1}.K^{-1}$ for the sandy soil and 0.51 to 0.78 $W.m^{-1}.K^{-1}$ for franco soil.

Characterization of multiple thermophysical data through the TWI contributes to the thermophysical mapping of the soils of Paraná and will allow in the future to draw a correlation with their respective bases analyzing the data via remote sensing, for example. Fluctuations of thermal parameters impact on all microbial activity of soils. Carbon dioxide concentration changes when the soil presents different temperatures [43]. Higher temperatures reduce the microbial activity of bacteria and fungi and increase the diversity of microbial community structure. Thermophysical properties also affect the rates of metal oxides.

Results indicated that the thermal characteristics of soil substrates lead to significant diurnal variations in soil temperatures. Profile analyses conducted by the authors using computerized X-ray tomography have demonstrated temporal variations in the soils. Using the OPC photoacoustic technique, Mota and collaborators [44] measured red clays collected from 1.2 to 2.5 m deep, in soil of the state of Rio de Janeiro (Brazil), it was pressed by 9 ton and thermally treated in the temperature range 300 to 1100 ℃. Values of α_s were established between 1 to 4 x 10^{-7} $m^2.s^{-1}$.

Momose and Kasubuchi [25] measured the thermal conductivity from three types of soil (Soil Ando, Soil Red Yellowy and Sand Toyoura) all soils of clayey texture, where the air pressure was reduced during experiment and temperature vary from 10 to 75 °C. Thermal conductivity increased markedly under reduced air pressure, beyond a critical soil water content of 101 kPa. The maximum thermal conductivity for each soil obtained was 2 $W.m^{-1}.K^{-1}$, such as manganese and iron in soils. Structural transitions are also affected by soil temperature [45]. In the models used in the simulations of heat transfer and temperature in the daily and seasonal cycles the thermophysical properties of thermal diffusivity, thermal conductivity and thermal effusivity are of important contribution. Tang and coworkers [46] reported that due to increased temperature during aerobic incubation at a concentration of organic matter were extremely reduced in soil samples. Jelinkhova and coworkers [47] canvassed the thermal regime and hydric in green roofs in very thin coverings of soils.

Photoacoustic, Photothermal, Heat Transient and Gravimetric techniques proved to be efficient for determination of thermophysical parameters. It is important to note that these are non-destructive, accessible techniques with good precision. The values obtained in this study showed good agreement with those found in the literature. The specific heat measured in the experiments corresponded well to the nature of the soils.

Apparent densities of agricultural land, which are essentially the Latosols and Nitosols, are in the range from 1200 to 1700$Kg.m^{-3}$, and the apparent densities of sandy soils correspond in the average to 1650 $Kg.m^{-3}$ [36]. Apparent density of sandy found in the literature was 1750 $Kg.m^{-3}$ and the bulk density is equal to 2500 $Kg.m^{-3}$. Works in literature indicating that soils with apparent density superior than 1700 $Kg.m^{-3}$ have serious difficulties for penetration from the roots, germination seeds, development and growth of plants because aeration and fast water vessel, because the diffusion of oxygen and other gases are changed, raising carbon gas concentration in the root area, and soils with apparent density higher than 2000 $Kg.m^{-3}$ have the movement of water and transports of ions and nutrients fully inhibited.

The pursuit of sustainable practices has become increasingly important across various sectors, especially in construction and material industries. In this context, the thermal properties of materials such as thermal diffusivity, thermal conductivity, and thermal effusivity play a crucial role in energy efficiency and building sustainability [48]. This article explores the correlation between these thermal properties and sustainability, highlighting how understanding and applying these concepts can contribute in eco-friendly and economical practices.

Thermal conductivity is a material's ability to conduct heat. Materials with high thermal conductivity, such as metals, allow for rapid heat transfer, while materials with low thermal conductivity, such as foam, act as thermal insulators. In construction, choosing materials with low thermal conductivity can reduce the need for heating and cooling systems, thereby contributing to the energy efficiency of buildings and, consequently, to sustainability [49]. Thermal diffusivity measures how quickly heat spreads through a material. It is calculated from a material’s thermal conductivity, density, and specific heat. Materials with high thermal diffusivity respond rapidly to temperature changes, which can be advantageous in extreme climates by helping to regulate indoor temperatures and reducing the need for artificial heating or cooling. Thermal effusivity is the capacity of a material to absorb and release heat [50]. Materials with high thermal effusivity can efficiently store and release heat, which can improve indoor thermal comfort. In terms of sustainability, materials with high thermal effusivity can help moderate temperature fluctuations, reducing the need for climate control systems and thereby decreasing energy consumption.

Understanding thermal properties is fundamental to sustainable agricultural practices like crop management, where choosing species suited to soil thermal conditions can optimize production and reduce the need for external inputs. Also in soil conservation, practices such as mulching can help regulate temperature and humidity, improving soil health and biodiversity and regularization of the environment temperature change. In the last case, rising global temperatures can affect the thermal properties of soils, impacting agriculture and environmental conservation.

The study of soils with appropriate thermal properties is very important for constructing sustainable buildings. Thermal conductivity, diffusivity, and effusivity play key roles in energy efficiency and thermal comfort, directly impacting building sustainability. Investing in materials that optimize these properties can lead to significant reductions in energy consumption, helping to build a more sustainable future.

4 Conclusion

The search for alternative detection systems that offer agility and cost reduction for measurements, with sensitivity to characterize various types of soils, including those affected by burning with higher salt concentrations, soils in erosion stages, exposure to toxic waste and contaminants, and samples from different climates such as semi-arid, temperate, cold, and those subjected to ice accumulation from snow has consistently motivated researchers. These systems also aid in monitoring the treatment and revitalization of soils.

In this work the technique TWI using white light produced measurements of temperature fluctuation in soils of different textures and horizons, making possible the characterization of thermal diffusivity, thermal effusivity and thermal conductivity. The results presented by TWI showed that in sandy soils whose predominant mineral constitution is formed by SiO_2 and $Al_2Si_2O_5(OH)_4$, are more conductive and thermally diffusive than clayey soils, of which its predominant mineral constitution are oxides Fe_2O_3 and FeO(OH). The increase in the thermal transport properties of the soils did not follow the same proportion as the predominant minerals. This is due to the presence of other secondary and primary minerals that also compose the soil, as well as the incorporation of existing organic matter in the porous fraction. Results indicated that in the surface horizon layer, poor in organic matter, the thermal diffusivity and thermal conductivity were lower than that in deeper horizons (subsurface). This result is important because it indicates that the heat tends to be distributed faster in soil surface rather than in bulk extracts. Samples were submitted to the same temperature change on the soils, which was about 2K in tests. Gravimetric measurements were also made to estimate the bulk and particle densities and gravimetric humidity from Parana soils. Pipette method was used to auxiliary in the soil densities identification. Bulk density and particle density of clayey soils were about 1350Kg.m^{-3}, and from 2300 to 2500Kg.m^{-3}, respectively. Soils bulk density sandy and medium sandy textures varied from 1400 to 1900 Kg.m^{-3} and the particle density had range from 2500 to 2700 Kg.m^{-3}. Lower-density soils are more porous because of their big cohesion of clay grains. By the bulk density measurements and heat specific by Thermal Relaxation method, it was possible to calculate the product of the volumetric thermal capacity and link it with the values achieved through TWI. Finally, the OPC system was used to measure soils as close as possible “in natural powder form” and characterize the thermal diffusivity of the Argisols in the horizons HA and HB. Results showed that the Argisols thermal diffusivity was smaller than 10^{-7} m^2.s^{-1}. Data obtained for the thermophysical characterization of soils are related to simulations in heat transfer and water transfer models. This analysis examines the contribution of temperature to various soils, the effects

of organic material on temperature, and thermal anomalies in auxiliary soils. Additionally, it includes the generation of images through remote sensing for studies in various fields of knowledge.

References

1. Franck-Néel, C., Borst, W., Diome, C., Branchu, P. (2015). Mapping the land use history for protection of soils in urban planning: what reliable scales in time and space. *J Soils Sediments* 15:1687–1704.
2. Pinheiro, E. F. M., Ceddia, M. B., Clingensmith, C. M., Grunwald, S., Vasques, G. M. (2017). Prediction of Soil and Chemical Properties by Visible and Near – Infrared Diffuse Reflectance: Spectroscopy in the Central Amazon. *Remote Sensing*. 9(4), 293.
3. Kharaka, Y. K and Dorsey, N. S, (2005). Environmental issues of petroleum exploration and production: *Introduction*, *Environ Geoscience*, 12 (2), 61-63.
4. Dominguez Hernandez, M. E., Dominguez-Hernandez, E., Martinez-Barrera, G., Dominguez-Hernandez, A., and Zepeda-Bautista, R. (2022). Transdisciplinary Interventions to Improve the Sustainability of Maize Agroecosystems: A Case Study from Mexico. *Transdisciplinary Journal of Engineering & Science*, *13*. https://doi.org/10.22545/2022/00196.
5. Ben-Dor, E., Chabrillat, S., Demattê, J. A. M., Taylor, G. R., Hill, J, Whiting, M. L., Somme, S. (2009). Using Imaging Spectroscopy to study soil properties. *Remote Sens Environ*. 113:538–555.
6. Hernandez-Aguilar, C., Saucedo-Alfonzo, D. A., Dominguez-Pacheco, A., Valderrama-Bravo, M. del C., Igno Rosario, O., Valencia-Hernandez, J. E., Mundo-Franco, Z., Ivanov-Tsonchev, R., and Martinez-Ortiz, E. J. (2023). The Transdisciplinarity for Sustainable Development: Incorporating Organic Waste into Bread-Making. *Transdisciplinary Journal of Engineering & Science*, *14*. https://doi.org/10.22545/2022/00227.
7. Anjaneya Babu Padavala, S. S. and Potharaju, M. (2022). Performance Evaluation of Mechanical and Durability Properties of Fly Ash and Silica Fume Based Concrete for Sustainable Building Material. *Transdisciplinary Journal of Engineering & Science*, *13*. https://doi.org/10.22545/2022/00183.
8. Entwistle, J. A. and Abrahams, P. W. (1997). Multi-element analysis of soils and sediments from Scottish historical sites. The potential of inductively coupled plasma-mass spectrometry for rapid site investigation. *Journal of Archaeological Science*, *24*(5), 407-416.
9. Richter, D. D. and Yaalon, D. H. (2012). The Changing Model of Soil Revisited, *Soil Science Society of America Journal. 76, 766-778.*
10. Liu, R., Chen, D., Hayden, H., He, J., Suter, H., (2015). Influence of temperature and moisture on the relative contributions of heterotrophic and autotrophic nitrification to gross nitrification in an acid cropping soil. *Journal Soils Sediments*. 15 (11), 2304-2309.
11. Wang, Y., Gao, S., Li, C., Zhang, J., Wang, L. (2016). Effects of temperature on soil organic carbon fractions aggregate stability and structural characteristics of humid substances in a Mollisol. *Journal Soils Sediments*. 16 (7), 1849-1857.
12. Schaeffer, A., Nannipieri, P., Kästner, M., Schmidt, B., Botterweck, J. (2015). From humic substances to soil organic matter – microbial contributions. In honor of Konrad Haider and James P. Martin for their outstanding research contribution to soil science. *Journal Soils Sediments*. 15 (9), 1865-1881.

13. Lal, R., (2015). Restoring soil quality to mitigate soil degradation. *Sustainability*, 7(5), 5875-5895.
14. Kumar, S. and Singh, R. (2014). Soil management for sustainable agriculture: *An* Agronomy *for Sustainable Development*, 34(3), 491-511.
15. Jones, R. J. and Smith, P. (2013). The impact of soil properties on climate change mitigation strategies. *Global Change Biology*, 19(5), 1591-1600.
16. Wang, J. and Zhang, L. (2012). The role of thermal effusivity in the sustainability of agricultural systems. *Agricultural Water Management*, 108, 7-14.
17. Silva, M. L. D., Silva, A. C., Silva, B. P. C., Barral, U. M., Soares, P. G., and Vidal-Torrado, P. (2013). Surface mapping, organic matter and water stocks in peatlands of the Serra do Espinhaço Meridional-Brazil. *Revista Brasileira de Ciência do Solo*, *37*, 1149-1157.
18. Cezar, E., Nanni, M. R., Demattê, J. A. M., Chicati, M. L., and Oliveira, R. B. D. (2013). Estimation of soil properties by means of diffuse spectroradiometry. *Revista Brasileira de Ciência do Solo*, *37*, 858-868.
19. Bennet, C. A. and Patty, R., (1982). Thermal wave interferometry: a potential application of the photoacoustic effect, *Applied optics*, 21 (1), 49-54. doi: 10.1364/AO.21.000049. PMID: 20372398.
20. Almond, D. and Patel, P., (1996). *Photothermal Science and Techniques*. London: Chapman and Hall.
21. Rosencwaig, A. and Gersho, A. (2008). Theory of the photoacoustic effect with solids, *Journal Applied Physics*, 47, 64.
22. Mariucci, V. V. G., da Cruz, J. A., Bonadio, T. G. M., Picolloto, A. M., Weinand, W. R., Lima, W. M., Medina, A.M. and Bento, A. C. (2015). Effective Thermal Diffusivity Study of Powder Biocomposites via Photoacoustic Method. *Brazilian Journal of Physics*, *45*, 525-531.
23. Medina, A. N., Caldeira, A., Bento, A. C., Baesso, M. L., Sampaio, J., Catunda, T., and Gandra, F. G. (2002). Thermal relaxation method to determine the specific heat of optical glasses. Journal of Non-Crystalline Solids, 304(1-3), 299-305. https://doi.org/10.1016/s0022-3093(02)01038-4.
24. Barucci, M., Brofferio, C., Giuliani, A., Gottardi, E., Peroni, I., Ventura G. (2001). Measurement of Low Temperature Specific Heat of Crystalline TeO_2 for the Optimization of Bolometric Detectors, *Journal Low Temperature Physics*. 123 (5-6), 303-314.
25. Momose, T. and Kasubichi, T. (2002). Effect of reduced air pressure on soil thermal conductivity over a wide range of water content and temperature, *European Journal Science*, 53, 599-606.
26. Manhaes, R. S. T., Alexandre, J., Auler, L.T., Carrio, J. G., Garcia-Quiroz, A., Massunaga, M. S. O., Santos, D. R., Sthel, M. S., da Silva E. C., Vargas, H. (2002). Soil characterization using X-ray diffraction, photoacoustic spectroscopy and electron paramagnetic resonance. *Applied Clay Science*. 21, 303-311.
27. Bristow, K. L., Horton, R., Kluitenberg, H. J., (1994). Measurement of Soil Thermal Properties with a Dual-Probe Heat-Pulse *Technique, Soil Science Society of America Journal*, 58 (5), 1288-1294.
28. Bristow, K. L., Fitzgerald, T. S., Goding, C. J., Kluitenberg, G. J., (2001). A small multi-needle probe for measuring soil thermal properties, water content and electrical conductivity, *Computers and Electronics in Agriculture*, 31 (3), 265-280.
29. Amin, S., Chen, C., Ghadiri, H., Marschner, P. (2016). Salt-affected soils, reclamation, carbon dynamics, and biochar: a review. *Journal Soils Sediments*. 16, 939-953.

30. Ciarkowska, K. (2017). Organic matter transformation and porosity development in non-reclaimed mining soils of different ages and vegetation covers: a field study of soils of the zinc and lead ore area in SE Poland. *Journal Soils Sediments*, 17, 2066–2079.
31. Xuezhang, L., Xianli, X., Liu, W., Xu, C., Zhang, R., Wang, K. (2017). Prediction of profile soil moisture for one land use using measurements at a soil depth of other land uses in a karst depression. *Journal Soils Sediments*., 16, 939-953.
32. Wang, Y. Q., Hu, W., Zhu, Y.J., Shao, M.A., Xiao, S., Zhang, C.C. (2015). Vertical distribution and temporal stability of soil water in 21 m profiles under different land uses on the Loess Plateau in China. *Journal Hydrology*, 527, 543-554.
33. Coelho, T. M., Nogueira, E. S., Lima, W. M., Medina, A. N., Steimacher, A., Weinand, W. R., Baesso, M. L., Bento, A. C., (2007). Thermal properties of natural nanostructured hydroxyapatite extracted from fish bone waste. *Journal Applied Physics*, 101, 084701 - 084711.
34. Picolloto, A. M., Astrath, N. G. C., Astrath, F. B. C., Baesso, M. L., Mariucci., V. V. G., Medina, A. N., Moraes, J. C., Santos, A. D., Szpak, W., Bento, A. C. (2013). Non-destructive thermal wave method applied to study thermal properties of fast setting time endodontic cement, *Journal Applied Physics*, 114: 194701- 194701-10.
35. de Vries, D.A. and Peck, A.J. (1958). On the Cylindrical Probe Method of Measuring Thermal Conductivity with Special Reference to Soils. II. Analysis of Moisture Effects. *Australian Journal of Physics* 11, 409-423. https://doi.org/10.1071/PH580409.
36. Barik, K., Canbolat, M., Islam, K. R., Yanik, Y. R., (2011). Compressive behavior of soils as affected by aggregate size with differences texture in Turkey. *Journal of Animal and Plant Sciences*. 21 (2), 186-192.
37. Waheham, S. G. and Canuel, E. A., (2016). The nature of organic carbon in density-fractionated sediments in Sacramento – San Joaquim River Delta (California). *BIOGEOSCIENCES*, 13, 567-582.
38. Silans, A. P., Silva, F. M., Barbosa, F. A. R. (2006). Determinação in loco da difusividade térmica num solo da região de caatinga (Pb), *R. Bras. Ci. Solo*, 30, 41-48.
39. Bodzenta, J., Kaźmierczak-Bałata, A., and Mazur, J. (2010). Photothermal methods for determination of thermal properties of bulk materials and thin films. *Central European Journal of Physics*, *8*, 207-220.
40. Nicolau, J., Rivez A. J. F., Debbaut, V., (1993). Thermal conductivity measurements in soil using an instrument in the cylindrical probe method. *Review of Scientific Instruments*, 64 (3), 774-780.
41. Carvalho, J. L. N., Raucci, G. S., Cerri, C. E. P., Bernoux, M., Feigl, B. J., Wruck, F. J., and Cerri, C. C. (2010). Impact of pasture, agriculture and crop-livestock systems on soil C stocks in Brazil. *Soil and Tillage Research*, *110*(1), 175-186.
42. Nusier, O. K. and Habuhamed, N. H., (2003). Laboratory Techniques to evaluate thermal conductivity for some soils. *Heat* and *Mass Transfer*, 39 (2), 119-123.
43. You, G., Zhang, Z., Zhang, R. (2018). Temperature adaptability of soil respiration in short-term incubation experiments, *Journal Soils Sediments*, 19, 557-565.
44. Mota, L., Faria. R. T., Holanda, J.N.F., Machado, F.A.L., Toledo, R., Vargas, H., (2008). Thermal characterization of red clay from the Northern Region of Rio de Janeiro State, Brazil using an open photoacoustic cell, in relation to structural changes on firing, *Applied Clay Science*, 42 (1–2), 168-174.

45. Dorau, K., Papenfuß, S., & Mansfeldt, T. (2018). Temperature-dependent oxide removal from manganese-and iron oxide-coated soil redox bars. *Journal of soils and sediments*, *18*, 680-687.
46. Tang, S., Cheng, W., Hu, R., Nakajima, M., Guigue, J. Kimani, S. M., Sato, S., Tawaraya, K., Xu, X (2017). Decomposition of soil organic carbon influenced by soil temperature and moisture in Andisol and Inceptisol paddy soils in a cold temperate region of Japan. *Journal Soils Sediments*. 17, 1843-1851.
47. Jelinkova, V., Sacha, J. Dohnal, M., (2016). Thermal and water regime studied in a thin soil layer of green roof systems at early stage of pedogenesis, *Journal Soils Sediments,* 16, 2568–2579.
48. Pacheco, S. L. (2022). Energy Efficiency in Buildings: Thermal Properties of Materials and Sustainability, *Journal of Sustainable Building*, 12 (4), 102-119.
49. Smith, J. R., (2021). The Importance of Thermal Conductivity in Sustainable Construction, *Materials Science Review*, 34 (7), 456-470.
50. Johnson, M. A, (2020). Thermal Diffusivity and Effusivity: Impacts on Building Energy Efficiency, *Energy and Buildings*, 55, 153-162.

About the Authors

Antonio Carlos Bento: Graduate in Physics at Universidade Estadual de Maringa/UEM (1984), Master in Science (1987) and Doctoral in Science (1990) at Universidade Estadual de Campinas/SP/Brazil. Post-doc at Bath University/UK (1993-1994) in Photothermal Science, Thermal Waves and Microscopy. Full professor in Photothermal Science at UEM (since 2009). Head of Photothermal Group at UEM and with expertise in condensed matter, thermal properties of glass. polymer, ceramics, metal alloys and bioceramics. Fellow Research of Brazilian National Council/CNPQ and Consulting member of many specialized journals in condensed matter and state foundation for Science. Former Post Graduate Director at UEM (2014-2018). Advisor of dozens of Master and Doctoral students at UEM in photothermal characterization of materials.

Angela Maria Picolloto: Bachelor's degree in Physics from the State University of Maringá (2010), Master's degree in Physics from the State University of Maringá (2011) and PhD in Physics from the State University of Maringá (2016), Degree in Mathematics from the State University of Maringá (2022). He has experience in the area of condensed matter physics with an emphasis on optical and thermophysical phenomena. It works with the characterization of materials, dental cements, soils, essential oils and bioedible films produced with soy protein matrix. Worked with the development of experimental practices with the purpose of demonstrating physical phenomena for basic education.

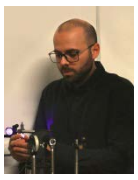

Vitor Santaella Zanuto: Adjunct Professor at the State University of Maringá (UEM - Paraná) and effective member of the Graduate Program in Physics at the same institution. Graduated in Physics Bachelor's Degree (2010), Master's (2012) and Doctorate (2015) in Condensed Matter Physics from the State University of Maringá. He participated in the Sandwich Doctorate Program Abroad (PDSE-CAPES) at Utah State University (USU - USA), under the supervision of Prof. Dr. Stephen E. Bialkowski. He carried out a Postdoctoral Internship in Physics at the University of

São Paulo (USP) at the Institute of Physics of São Carlos (IFSC), under the supervision of Prof. Dr. Tomaz Catunda. He has experience in the area of Condensed Matter Physics, working mainly in the following areas: Development and characterization of vitreous systems doped with optically active ions; Mechanical, thermal, structural, optical, and spectroscopic properties of crystalline and noncrystalline, organic and inorganic solids.

Danilo de Paula Kuritza: Bachelor's degree (2018) and master's degree (2020) in Physics from the State University of Maringá, currently a PhD student in Physics with a CAPES scholarship from the same university. He has experience in the area of Physics, with an emphasis on Condensed Matter Physics, working mainly on the following topics: Study of photoacoustic effects, with emphasis on photoacoustic spectroscopy (master's degree); Computational Physics, with emphasis on Simulation of two-dimensional nanomaterials, study of electronic, optical and structural properties through first principles methods.

Mauro Luciano Baesso: Full professor at the Physics Department of the State University of Maringá.Physicist-State University of Maringá (1984), MSc in Physics-IFGW-UNICAMP (1987), Ph.D. in Photoacoustic and Glass Science-IFGW-UNICAMP (1990). Post-Doctoral in Photothermal Science, Institute of Science and Technology (UMIST) - University of Manchester - UK (1994). Visiting Professor in Optoacoustic Imaging Science, ETH-Zurich (2020). Visiting Professor in Photothermal Imaging Science, Photon Science Institute - University of Manchester (2024). His WORK includes fundamental and applied research, and technological development in Photoacoustic and Photothermal Phenomena in Biological and Healthcare Science, Biomaterials for bone substitution, Optical Glasses for smart white lighting, Laser Sources and Solar Energy Devices, and Optical and Spectroscopy properties of Advanced Functional Material in multidisciplinary studies. Published 428 original papers, 2 book chapter, 2 filed patents, 2 applied patents, and advised ~74 theses and postdocs.

Marcos Rafael Nanni: PhD in Agronomy (Soils and Plant Nutrition) [Esalq] from the University of São Paulo in 2000. He is currently Full Professor of the Department of Agronomy at the State University of Maringá and Coordinator of the Postgraduate Course in Agronomy. He has published more than 70 articles in specialized journals and 80 papers in annals of events. He has 4 book chapters and 3 published books. It has 3 software and another 34 items of technical production. He participated in 8 events in Brazil and 3 abroad. He supervised 14 master's dissertations, 4 doctoral dissertations and 1 postdoctoral dissertation. He currently supervises 1 master's student and 6 doctoral students, in addition to having supervised 15 scientific initiation works and 30 course completion works in the areas of Agronomy, Geosciences, Agricultural Engineering, Geography and Environment.

Everson Cezar: Graduated in Agronomy with a master's, doctorate and postdoctoral degree in the area of soils and plant nutrition from the State University of Maringá. They have experience in the area of soil survey and classification, pedometry, precision agriculture and remote sensing applied to the study of soils. He is currently a professor of soils at the State University of Minas Gerais, Passos Unit, in the agronomy course, productivity scholarship holder, coordinator of the Study Group on Soils and Precision Agriculture - GESAP and the geology and geotechnics laboratory.